J. Fluid Mech. (1995), *vol.* 305, *pp.* 93–109
Copyright © 1995 Cambridge University Press

Two-dimensional vortex motion in the cross-flow of a wing–body configuration

By T. W. G. DE LAAT[1] AND R. COENE[2]

[1] Flight Test Department, Royal Netherlands Air Force, Binckhorstlaan 135, PO Box 20703, 2500 ES The Hague, The Netherlands

[2] Department of Aerospace Engineering, Delft University of Technology, Kluyverweg 1, PO Box 5058, 2600 GB Delft, The Netherlands

(Received 21 October 1994 and in revised form 6 July 1995)

For a two-dimensional potential flow, Föppl obtained the equilibrium positions for a symmetric vortex pair behind a circular cylinder in a uniform oncoming flow. In this article it is shown that such an equilibrium is in general possible for a vortex in a stagnation flow (e.g. in a corner). Furthermore it is found that a vortex near such an equilibrium position will rotate with a definite frequency around this equilibrium. Expressions are derived for the frequencies associated with the closed orbits of the vortices in the case of the equilibrium of a vortex in a stagnation flow and for the equilibrium of the symmetric vortex pair behind a circular cylinder in oncoming flow. For the large-amplitude case the vortex trajectories are calculated by using a fifth-order Runge–Kutta integration method. The analysis is then extended to the case of a simple wing–body combination in a cross-flow such as arises for a slender aircraft at an angle of attack with vortices generated by strakes or at the front part of the body. At the wing–body junctions the motions of the vortices may be periodic, quasi-periodic or the vortices may be swept away, depending on the initial conditions.

1. Introduction

In the design of modern aircraft, vortices are used to improve manoeuvrability at high angles of attack. The vortices may be generated at the forebody or at the intersection of wing and body by so-called strakes (figure 1). Despite numerous experiments and computational efforts the behaviour of such vortices in the neighbourhood of an aircraft is not fully understood. Especially, the occurrence of oscillating forces and vortex breakdown pose problems. The periodic and quasi-periodic flows discussed in this paper may be relevant to an explanation of such phenomena.

In order to obtain some insight into vortex flows around wing–body configurations it appeared natural to start with a study of simple two-dimensional incompressible potential flows with concentrated vortices in the neighbourhood of wing–body-like cross-sections which also arise in the usual slender-body approximation.

As described by e.g. Lamb (1932) and Saffman (1992), in 1913 Föppl investigated the case of a circular cylinder in a uniform oncoming flow, followed by a vortex pair 'symmetrically disposed with respect to the line of advance of the centre'. Using the method of images it is shown that the vortices can maintain their positions relative to the cylinder, provided they lie on a certain (symmetric) curve emanating from the rear stagnation point and that the strengths of the vortices (equal and opposite) correspond

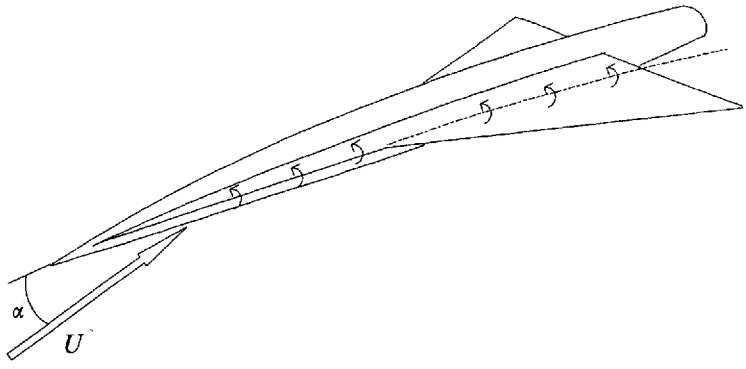

FIGURE 1. Vortex flow near a wing–body combination.

to a given position on this curve. The arrangement is known to be unstable for non-symmetrical disturbances and the vortices are then convected away from the cylinder. Apparently the equilibrium of the vortices is precarious. In the equilibrium situation with the vortices approaching the stagnation point on the cylinder, the flow in the near field is equivalent to the flow field of a vortex pair (symmetrically disposed) near a stagnation point on a flat wall or of a single vortex in a corner flow field. This case is discussed in §2, using the method of images. Small symmetric displacements of the vortices lead to small circular trajectories around the equilibrium positions with a definite frequency.

In §3 a similar analysis is applied to the case of a symmetric vortex pair near a circle. Periodic solutions are obtained with the vortices orbiting around Föppl's equilibrium points. The frequencies belonging to the Föppl equilibria are derived. For large but symmetric perturbations a fifth-order Runge–Kutta integration method is applied for calculating the vortex trajectories.

In §4 the cross-flow around a wing–body combination at an angle of attack is constructed by application of two successive Joukowski transformations. The vortex velocities are obtained analytically using a result due to Lin (1941). A vortex pair at the top of the body behaves in a way similar to that found in §3 for a circular cylinder. A vortex pair situated close to the wing-body junctions, however, gives rise to some new features. Equilibrium positions and the corresponding frequencies are calculated numerically. In addition to the periodic solutions with perfect left–right symmetry there are also solutions which are not symmetric and not periodic. It may also happen that one vortex is convected away, while the other one remains trapped and ultimately tends to move periodically.

2. A vortex in a corner flow field

To analyse the motion of a vortex of constant circulation Γ near a contour in a free flow we first consider the simple case of a vortex in a corner flow field. The velocity components u_1 and v_1, in the x- and y-directions respectively, of vortex 1 (with coordinates (x_1, y_1), figure 2) and the resulting vortex trajectories are well-known (e.g. Lamb 1932). The stagnation flow (e.g. Batchelor 1967) can be represented by $u = -kx$, $v = ky$, where k is a constant. For $k > 0$ the flow field is as shown in figure 3, where the streamlines are given by rectangular hyperbolae.

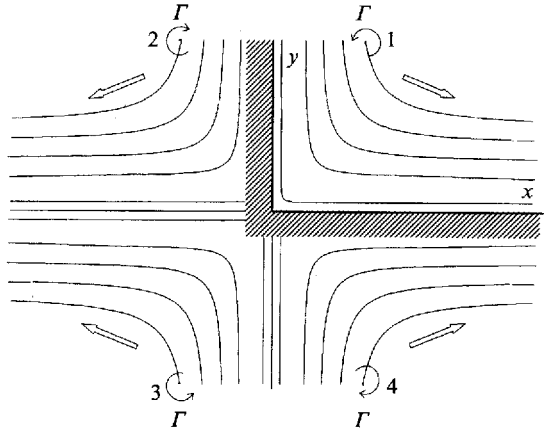

FIGURE 2. Trajectories of a vortex in a rectangular corner.

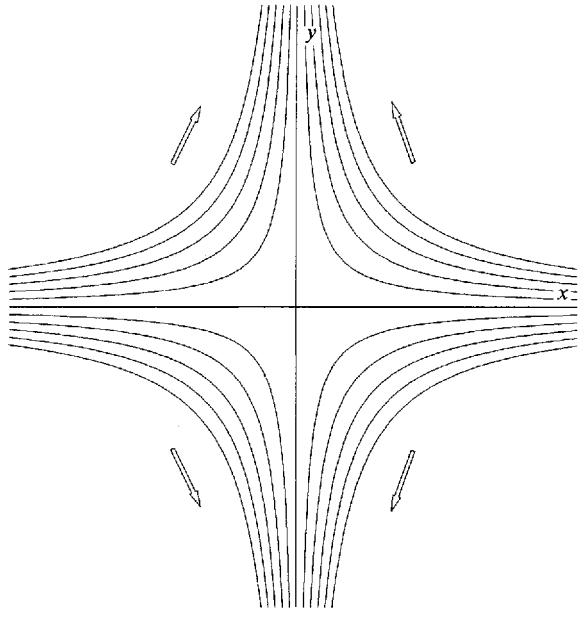

FIGURE 3. Streamlines of a flow field near a stagnation point.

For the combined flow field the velocity of vortex 1 is given by

$$\left.\begin{aligned} u_1 = \dot{x}_1 &= \frac{\Gamma}{4\pi y_1(x_1^2+y_1^2)} - kx_1, \\ v_1 = \dot{y}_1 &= -\frac{\Gamma}{4\pi x_1(x_1^2+y_1^2)} + ky_1. \end{aligned}\right\} \tag{1}$$

Solving (1) for $u_1 = v_1 = 0$ yields that (x_0, y_0) is an equilibrium point if

$$x_0 = y_0 \quad \text{and} \quad x_0 = \left(\frac{\Gamma}{8\pi k}\right)^{1/2}. \tag{2}$$

Stability

To investigate the stability we give the vortex and its mirror vortices a small displacement from the equilibrium position, which we denote as

$$\left.\begin{aligned} x_1 = x_0+\xi, \quad y_1 = y_0+\eta, \\ |\xi| \ll x_0, \quad |\eta| \ll y_0, \quad x_0 = y_0 > 0. \end{aligned}\right\} \tag{3}$$

The velocity of vortex 1 near its equilibrium position is obtained by substituting (3) into (1). Using (2) and neglecting second-order terms in ξ and η yields

$$u_1 = -\frac{\Gamma}{4\pi x_0^2}\eta, \quad v_1 = \frac{\Gamma}{4\pi x_0^2}\xi. \tag{4}$$

These equations represent a circular path round the equilibrium position, which can easily be seen by eliminating the time from (4): $\xi\,\mathrm{d}\xi+\eta\,\mathrm{d}\eta = 0$. Integration results in

$$\xi^2+\eta^2 = \text{const.}$$

Using (4) and (2) one finds that the circular trajectory has a constant angular velocity passing through it:

$$\omega = \frac{\Gamma}{4\pi x_0^2} = 2k, \tag{5}$$

which is independent of the radius of the trajectory, and of the distance of the equilibrium point to the stagnation point.

Another aspect of the motions considered here is revealed by taking a closer look at the derivatives. From (1), it follows that at the equilibrium point (a, a) we have

$$\left(\frac{\partial v_1}{\partial x_1}-\frac{\partial u_1}{\partial y_1}\right)_{(a,a)} = \frac{\Gamma}{2\pi a^2}. \tag{6}$$

Comparison of (6) with (5) shows that the 'vorticity' is twice the angular velocity, as might have been anticipated from the kinematics of vorticity fields (e.g. Lighthill 1986).

From (1) we also note that the field (u_1, v_1) is free of divergence, and one readily obtains a streamfunction, known as the Kirchhoff–Routh path function:

$$\psi_1(x_1, y_1) = \frac{\Gamma}{4\pi}\ln\frac{x_1 y_1}{(x_1^2+y_1^2)^{1/2}} - kx_1 y_1 = \text{const.}$$

At the equilibrium point we furthermore have, using (2),

$$\left(\frac{\partial u_1}{\partial x_1}\right)_{(a,a)} = \left(\frac{\partial v_1}{\partial y_1}\right)_{(a,a)} = 0. \tag{7}$$

Thus the equilibrium conditions (2) also lead the stagnation flow-field term and the contour-induced velocity term to compensate each other in these derivatives. From (7) one might conclude that the equilibrium is neutral, in the sense that a small displacement from the equilibrium position only causes a velocity perpendicular to the displacement vector and no velocity towards or away from the equilibrium.

3. A symmetric vortex pair near a circle

We now consider a vortex pair symmetrically disposed above a circular cylinder with radius a in an upward flow w as shown in figure 4. We use a complex plane with $\zeta = \xi+\mathrm{i}\eta$. The inner vortices are placed to satisfy the boundary condition on the circle.

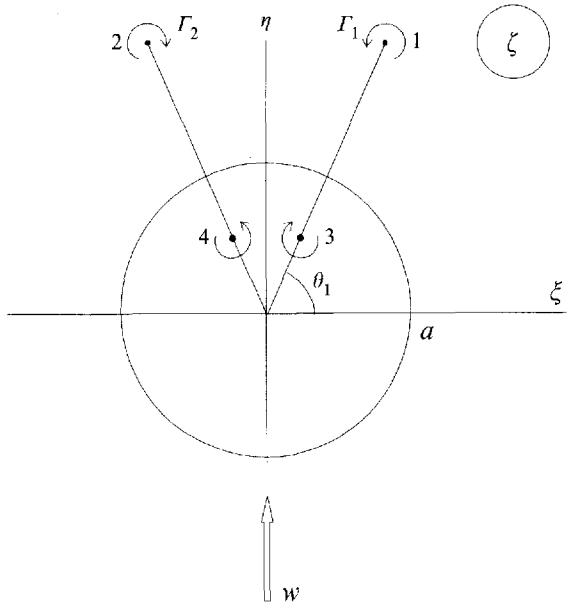

FIGURE 4. Symmetric vortex pair above a circular cylinder in upward flow (w).

This is a well-known flow field and the vortex velocity is easily obtained using complex functions and Helmholtz's theorem.

With $-\Gamma_1 = \Gamma_2 = \Gamma$, it follows from the velocity of vortex 1 that

$$u_1 - \mathrm{i}v_1 = \frac{\mathrm{i}\Gamma}{2\pi}\left\{\frac{1}{\zeta_1 - a^2/\overline{\zeta_1}} + \frac{1}{\zeta_1 + \overline{\zeta_1}} - \frac{1}{\zeta_1 + a^2/\zeta_1}\right\} - \mathrm{i}w(1 + a^2/\zeta_1^2). \tag{8}$$

For this symmetric case there are equilibrium point likes the equilibrium found in the previous section. This equilibrium was already derived by Föppl in 1913 (e.g. Lamb 1932 or Saffman 1992).

With $\zeta_1 = \zeta_0 = r_0 \mathrm{e}^{\theta_0 \mathrm{i}}$, Föppl found from (8) that there is equilibrium for (in our notation)

$$\cos\theta_0 = \frac{r_0^2 - a^2}{2r_0^2} \quad \text{and} \quad \frac{\Gamma}{2\pi} = w\frac{(r_0^2 - a^2)^2(r_0^2 + a^2)}{r_0^5}. \tag{9}$$

Beside this equilibrium there is also balance for

$$\theta_0 = 0 \quad \text{and} \quad \frac{\Gamma}{4\pi} = w\frac{(r_0^2 - a^2)(r_0^2 + a^2)^2}{r_0(r_0^4 + 4a^2 r_0^2 - a^4)}. \tag{10}$$

3.1. *Limiting value of the frequency of the equilibrium of a symmetric vortex pair above a circular cylinder in upward flow*

As in §2 we determine the vortex velocity in the neighbourhood of the Föppl equilibrium position by giving the vortex a small displacement from its equilibrium position. The position of the vortex 1, $\zeta_1 = r_1 \mathrm{e}^{\theta_1 \mathrm{i}}$ is substituted in (8) with

$$r_1 = r_0 + \delta, \quad \theta_1 = \theta_0 + \alpha, \quad \delta \ll r_0, \quad |\alpha r_0| \ll r_0.$$

This yields local Cartesian coordinates δ and $r_0\alpha$ near the equilibrium positions as

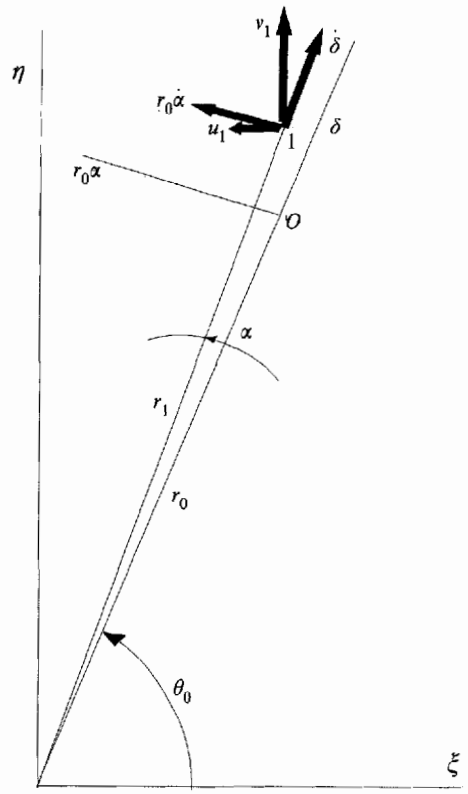

FIGURE 5. Transformation of coordinates.

shown in figure 5. Neglecting quadratic terms in δ and $r_0\alpha$ and eliminating the terms for the zero velocity in the equilibrium position and using (9) to simplify, one obtains

$$\left.\begin{aligned} u_1 &= -\frac{wa^2}{r_0^5}\{(r_0^2+3a^2)\,\delta\sin\theta_0+(3r_0^2-a^2)\,r_0\alpha\cos\theta_0\},\\ v_1 &= \frac{w}{r_0^5}\{(2r_0^4+a^2r_0^2+3a^4)\,\delta\cos\theta_0-(2r_0^4+3a^2r_0^2-a^4)\,r_0\alpha\sin\theta_0\}. \end{aligned}\right\} \tag{11}$$

We now decompose the velocity in the directions δ and $r_0\alpha$. As indicated in figure 5 we have

$$\dot{\delta}\approx u_1\cos\theta_0+v_1\sin\theta_0,\quad r_0\dot{\alpha}\approx -u_1\sin\theta_0+v_1\cos\theta_0,$$

which, upon substitution of (11) yields

$$\left.\begin{aligned} \dot{\delta} &= \frac{w}{r_0}\left\{\delta\sin 2\theta_0+r_0\alpha\frac{(a^2-3r_0^2)(3a^2+r_0^2)}{2r_0^4}\right\},\\ r_0\dot{\alpha} &= \frac{w}{r_0}\left\{\delta\frac{7a^4+r_0^4}{2r_0^4}-r_0\alpha\sin 2\theta_0\right\}. \end{aligned}\right\} \tag{12}$$

This is a system of two first-order linear differential equations with constant coefficients which can be solved using the method of eigenvalues. Putting

$$\begin{pmatrix}\delta\\ r_0\alpha\end{pmatrix}=\xi\,e^{\lambda t}$$

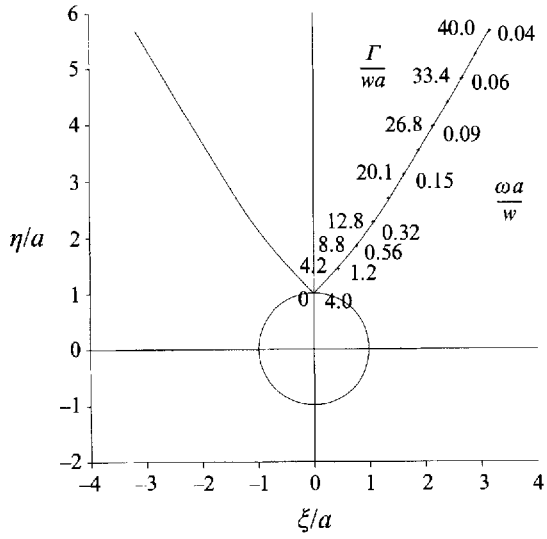

FIGURE 6. Plot of the dimensionless frequency along the equilibrium line.

and solving system (12) it is found that the system has only imaginary eigenvalues λ. After simplification (using (9)) one obtains that the purely periodic motion has the angular velocity

$$\omega = \frac{wa}{r_0^2}\left[\left(3-\frac{a^2}{r_0^2}\right)\left(1+2\frac{a^2}{r_0^2}+5\frac{a^4}{r_0^4}\right)\right]^{1/2}. \tag{13}$$

The fact that the real part of the eigenvalues equals zero means that we have the same kind of neutral equilibrium as in the rectangular corner flow field. There is only a periodic motion around the equilibrium position.

We note from (13) that for the limit case

$$\lim_{r_0 \to a} \omega = 4w/a.$$

This limit frequency is the same as the frequency of the equilibrium of a vortex in a rectangular flow field (5). This is true for $k = 2w/a$, and this is indeed the constant for the local stagnation flow field we find by applying a local approximation to the stagnation flow above the circular cylinder.

In figure 6 the dimensionless frequency $\omega a/w$ is plotted along the Föppl equilibrium line.

3.2. *Vortex trajectories*

To illustrate the derived equilibria and the vortex trajectories around them, vortex trajectories are calculated and drawn, starting with the vortices in a certain initial position. The vortex velocity is calculated using (8) and is integrated by means of a fifth-order Runge–Kutta integration method (with a certain time step Δt), which yields the position of the vortices after time step Δt. Repeating these calculations a number of times, the trajectories in the cross-plane are drawn for a symmetric initial disposition. With $w = 0$ we get the trajectories of figure 7(*a*). With (for example) $w = \Gamma/2a$, however, closed trajectories are formed, as drawn in figure 7(*b*). Note that because the time step Δt is constant, the distance between the points is a measure of the vortex speed.

The same mechanism as described in §2 leads to the closed trajectories of figure 7(*b*).

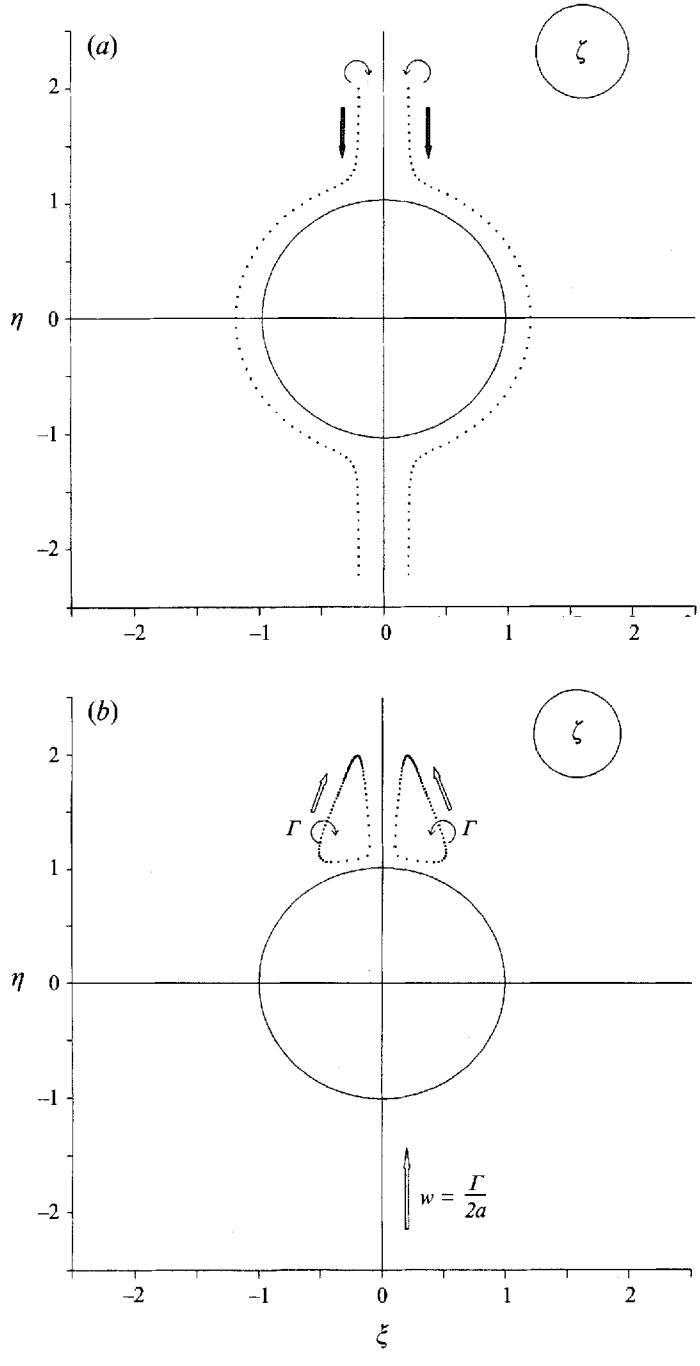

FIGURE 7. Trajectory of a symmetric vortex pair: (*a*) without upwash ($w = 0$), (*b*) with upwash $w = \Gamma/2a$. Initial positions (± 0.2, 2.0).

Between the stagnation point at (0, 1) and the equilibrium point, the vortex-induced vortex velocity dominates. But when the vortex is further away from the stagnation point the velocity of the free flow is stronger, and the vortex is convected with the free flow. When the two free vortices are close to each other, they will force each other back to the contour. The result of the two opposing contributions is that the vortices

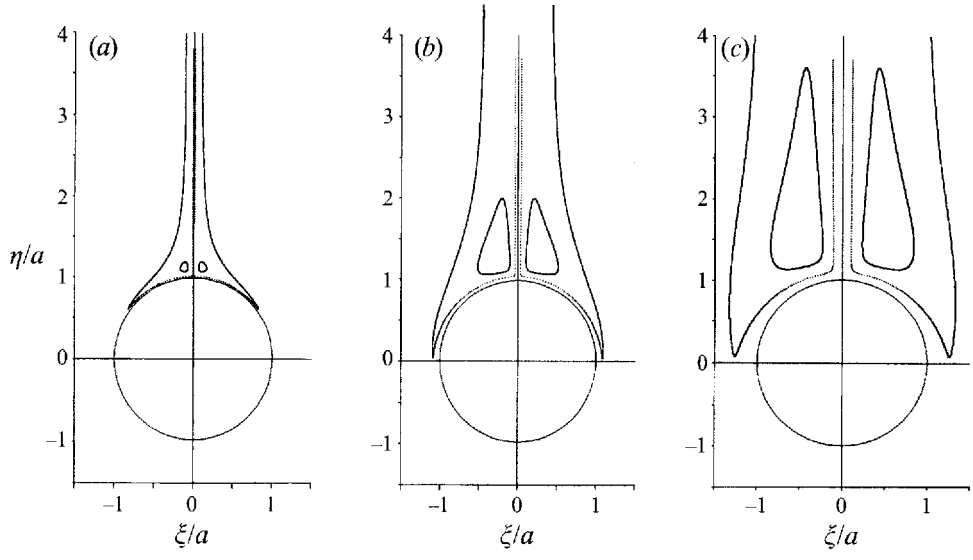

FIGURE 8. The regions of closed trajectories for three values of Γ/wa: (*a*) 0.5, (*b*) 2, (*c*) 5.

describe closed trajectories as drawn in figure 7(*b*). The Föppl equilibrium positions (for this Γ/wa) are situated in the centres of the closed trajectories.

The trajectories to the left are clockwise, while the trajectories to the right are counter-clockwise. It is noted that the vortex sign and the sense of the orbiting motion are the same: they are co-rotating. By reversing the signs of both w and Γ, the direction of the trajectories will be reversed.

To give some insight into the trapped regions, the trajectories tending to border the trapped regions and one inner trajectory are drawn for three values of Γ/wa in figure 8. The boundary trajectories go through the equilibrium on the horizontal axis (10). Of course the trajectories can be mirrored in the horizontal axis. Calculating the equilibrium positions on the horizontal axis from (10), one finds respectively $r_0 = x_0 = 1.020$, $r_0 = x_0 = 1.089$, $r_0 = x_0 = 1.261$. As we can see in the figure this equilibrium is obviously a saddle point.

One should remember that for the flow field of the symmetric free vortex pair above a cylinder in an upward uniform flow, closed trajectories can only be obtained when the flow field is symmetric. Non-symmetric disturbances are not allowed, which is shown later in this section. Symmetry can physically be enforced by putting a splitter plate on the vertical axis.

3.3. *Non-symmetric case*

As stated in Lamb (1932) Föppl was aware that the equilibrium is unstable for antisymmetric disturbances. This is verified by computations of the trajectories using a non-symmetrical formulation. The vortices are given small non-symmetric displacements from the equilibrium positions and an example of the resulting trajectories is plotted in figure 9.

It appears that because of the non-symmetrically disturbed equilibrium, one vortex is soon convected away with the free flow, and as a result the other one of course follows. The two vortices need each other (in symmetric position) to maintain the equilibrium. A small non-symmetric distortion will cause them to be successively convected with the free flow, away from the body, and away from the stagnation point. A similar situation arises for vortices which are not quite equally strong but initially

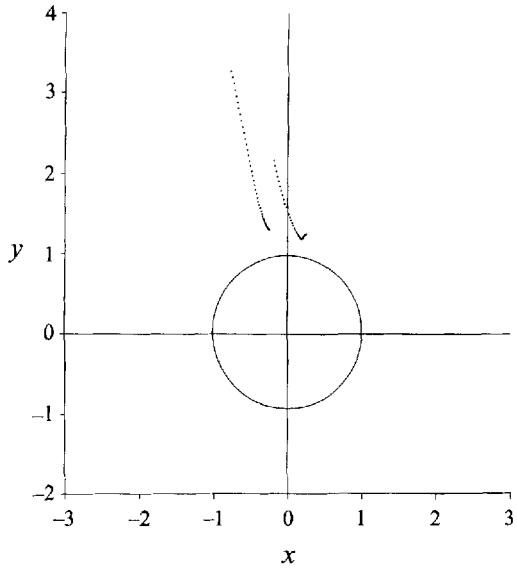

FIGURE 9. Vortex trajectory after a small asymmetric position–disturbance from equilibrium, for $\Gamma = 2$, $w = 1$ (with $\Delta t = 0.1$).

symmetrically diposed. At large distances from the cylinder however, such vortex pairs describe cycloïdal trajectories.

4. Vortex trajectories near a wing–body combination

The flow field near a simple wing–body combination can be found by successively applying two Joukowski transformations to the flow field round a circle (figure 10). The Joukowski transformations are

$$\zeta^* = \zeta + a^2/\zeta \quad \text{and} \quad \zeta^* = z + c^2/z.$$

Eliminating ζ^*:

$$\zeta = \tfrac{1}{2}(z + c^2/z + [(z + c^2/z)^2 - 4a^2]^{1/2}). \tag{14}$$

The flow field in the ζ-plane is given by

$$\chi(\zeta) = \frac{i\Gamma_1}{2\pi}\ln\frac{\zeta - a^2/\overline{\zeta_1}}{\zeta - \zeta_1} + \frac{i\Gamma_2}{2\pi}\ln\frac{\zeta - \zeta_2}{\zeta - a^2/\overline{\zeta_2}} - iw\left(\zeta - \frac{a^2}{\zeta}\right). \tag{15}$$

With the positions of the vortices in the ζ-plane we now calculate the velocities in the z-plane using the transformation

$$\overline{\dot{z}_1} = \left(\frac{d\chi}{dz}\right)_{z=z_1} = \left(\frac{d\chi}{d\zeta}\frac{d\zeta}{dz}\right)_{z=z_1}, \tag{16}$$

where z_1 is the position of vortex 1 in the z-plane. The vortex velocity is calculated by substitution of the vortex coordinates in the velocity equation, while discarding the infinite self-induced term. The vortex position is to be substituted in the velocity equation (16) with (15) for χ. But now we cannot simply discard the infinite self-induced part, because in combination with the transformation we find near the vortex position in the z-plane, using Taylor expansions:

$$\lim_{\epsilon \to 0} \frac{(d\zeta/dz)_{z=z_1+\epsilon}}{\zeta(z_1+\epsilon) - \zeta(z_1)} = \frac{1}{2}\frac{d^2\zeta/dz^2)_{z=z_1}}{(d\zeta/dz)_{z=z_1}},$$

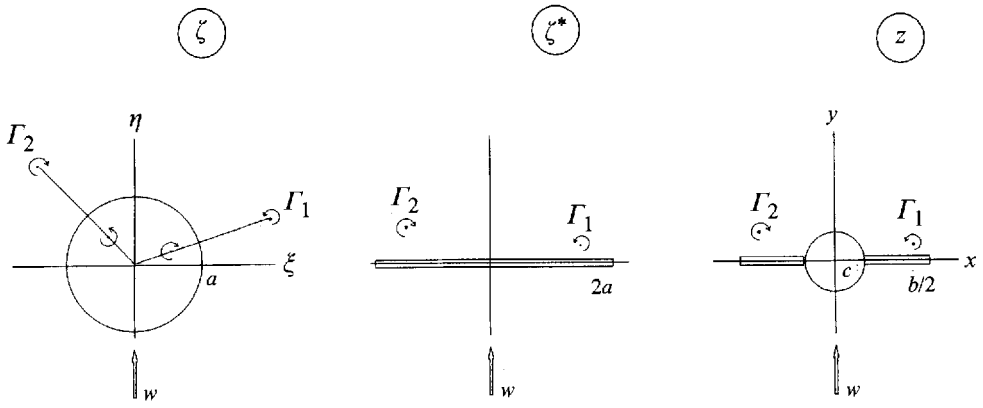

FIGURE 10. Transformation of the flow field round a circle to the flow field of a wing–body combination with span $b = 2\,(a+(a^2-c^2)^{1/2})$.

where ϵ is a small displacement. For the vortex velocity in the z-plane one finds

$$u_1 - \mathrm{i}v_1 = \left\{\frac{\mathrm{d}\chi}{\mathrm{d}\zeta} + \frac{\mathrm{i}\Gamma_1}{2\pi}\frac{1}{\zeta-\zeta_1}\right\}_{\zeta=\zeta_1} (\zeta')_{z=z_1} - \frac{\mathrm{i}\Gamma_1}{4\pi}\left(\frac{\zeta''}{\zeta'}\right)_{z=z_1} \tag{17}$$

with

$$\zeta' = \frac{\mathrm{d}\zeta}{\mathrm{d}z} \quad \text{and} \quad \zeta'' = \frac{\mathrm{d}^2\zeta}{\mathrm{d}z^2}.$$

This equation was first derived by Lin (1941).

Again the Runge–Kutta integration method is used to calculate the vortex trajectories with the expression for the vortex velocity, which is obtained by substituting (15) and the derivatives of transformation (14) in (17).

4.1. *Symmetric trajectories*

In figure 11, five trajectories are drawn for a symmetric vortex pair near a wing–body combination in an upward flow (see figure 10, z-plane, with $-\Gamma_1 = \Gamma_2 = \Gamma$) for $\Gamma/w = 2$, $c = 1$ and $a = 2$. The trajectories are drawn by choosing five different initial positions and plotting the resulting trajectories in one figure. The trajectories are symmetric about the vertical axis because the initial vortex positions are so chosen. As in §§2 and 3 the trajectories on the left are clockwise, while the trajectories on the right are counter-clockwise. The vortices move in the same direction; they are co-rotating.

From figure 11 one can see that for this case there are equilibrium positions near the stagnation point at the top, but also near the stagnation points at the intersection of wing and body. These equilibrium points are in the centres of the small closed trajectories. It is further noted that there are also equilibrium points on the positions where the trajectories around the two centres (in one quadrant) merge. In figure 11 these equilibrium points are situated where the upward part of the smallest trajectory drawn around two centres closely approaches the downward part. The equilibrium situated there is a saddle point. When a vortex pair is symmetrically disturbed from this equilibrium it will, depending on the direction of the distortion, either start to move around one of the two centre-like equilibria or it will follow a trajectory around both centres.

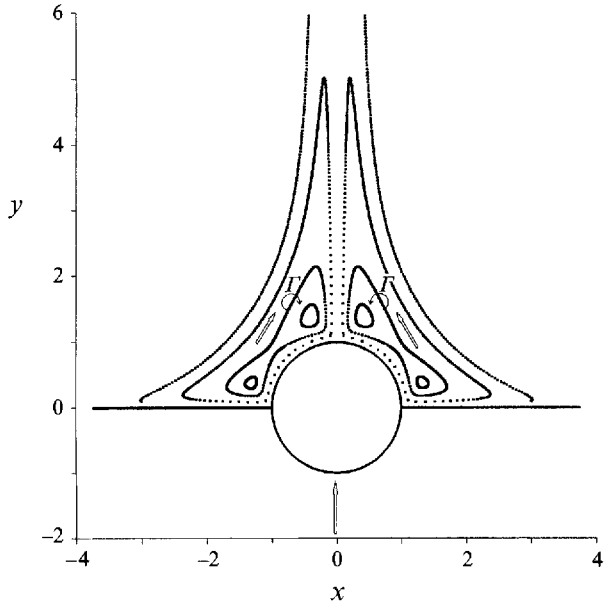

FIGURE 11. Symmetric vortex trajectories for $\Gamma/w = 2$, $c = 1$ and $a = 2$.

4.2. *Approximation of the frequency and equilibrium position in the corner*

The flow field due to the upward flow (w) in the z-plane of figure 10 is described by

$$u - \mathrm{i}v = \frac{\mathrm{d}\chi}{\mathrm{d}\zeta}\frac{\mathrm{d}\zeta}{\mathrm{d}z} = -\frac{\mathrm{i}w}{2}\left(1+\frac{a^2}{\zeta^2}\right)\left(1-\frac{c^2}{z^2}\right)\left(1+\frac{z+c^2/z}{[(z+c^2/z)^2-4a^2]^{1/2}}\right). \tag{18}$$

We make a local approximation of the stagnation flow field in the corner at the junction of wing and body by substituting:

$$z = c+\epsilon \quad \text{with} \quad |\epsilon| \ll c,$$

which yields to leading order

$$u - \mathrm{i}v = -\frac{2w\epsilon}{(a^2-c^2)^{1/2}}. \tag{19}$$

This has again the form of a stagnation-point flow field as defined in §2 but now with

$$k = \frac{2w}{(a^2-c^2)^{1/2}}.$$

With the relation between a, c and the span $b = 2[a+(a^2-c^2)^{1/2}]$ (figure 10), k is expressed in terms of the body radius c and span b:

$$k = \frac{8bw}{b^2-4c^2}.$$

The angular velocity follows by substituting this k into (5):

$$\omega = 2k = \frac{16bw}{b^2-4c^2}. \tag{20}$$

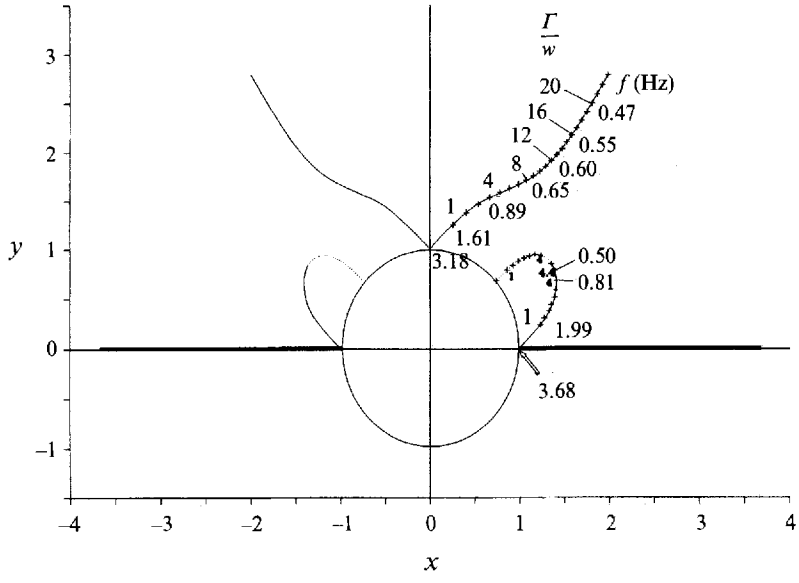

FIGURE 12. Equilibrium positions and the corresponding frequencies ($a = 2$ and $c = 1$), for $w = 10$.

The equilibrium position is obtained by substituting (20) in (2):

$$x_0 = \left(\frac{\Gamma}{4\pi\omega}\right)^{1/2} = \frac{1}{8}\left(\frac{\Gamma}{\pi b w}(b^2 - 4c^2)\right)^{1/2}, \tag{21}$$

and $y_0 = x_0$.

This approximation for the equilibrium position applies for $|x_0| \ll c$. For an aircraft with a circular body with radius c and wingspan b (figure 10) in an upward flow $w = U\sin\alpha$ (figure 1) we now have, for a certain Γ/w, an approximation for the equilibrium position of a vortex (Γ) in the corner flow field. The angular velocity for this equilibrium is approximated by (20).

In the same way for the equilibrium on the top of the body one finds $k = 2w/a$. Thus we have

$$\omega = 4\frac{w}{a} = \frac{16bw}{b^2 + 4c^2} \quad \text{and} \quad x_0 = \frac{1}{8}\left(\frac{\Gamma}{\pi b w}(b^2 + 4c^2)\right)^{1/2}, \tag{22}$$

x_0 being measured from the upper stagnation point.

4.3. *The equilibrium positions and their frequencies*

To plot the equilibrium positions and the corresponding frequencies the earlier described computer program for plotting the trajectories was used. The equilibrium positions were calculated numerically for a certain Γ/w. Then the vortex was placed near the equilibrium position (about 0.001 away); the closed trajectory that resulted was used to calculate the time period by multiplying the number of time steps by the magnitude of the time step. The results are shown in figure 12. It is emphasized that the equilibrium positions are determined by Γ/w, but that the magnitude of the frequency at an equilibrium position depends on the magnitude of w only. Furthermore figure 12 is plotted for flow fields symmetric about the vertical axis. The limit frequencies at the stagnation points of the corner (20) and on the top (22) are plotted as well. The lower equilibrium position disappears when Γ/w is greater than 4.4997. The saddle-like equilibrium and the lower neutral equilibrium then merge. A trajectory

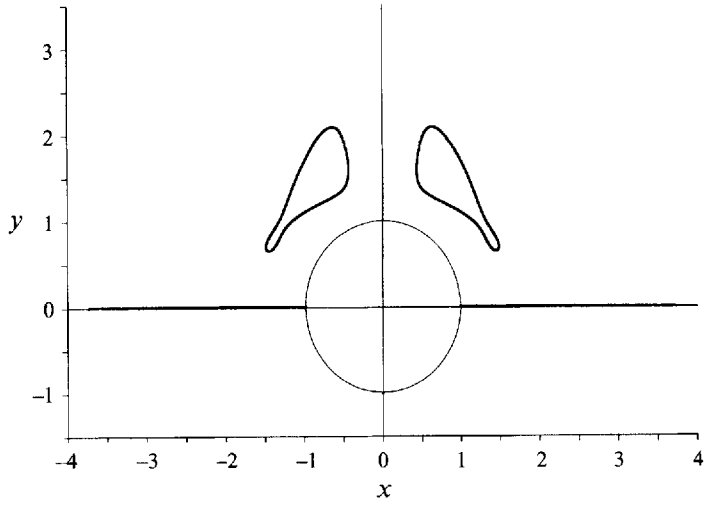

FIGURE 13. Vortex trajectory near the lower equilibrium for $\Gamma/w = 4.4$.

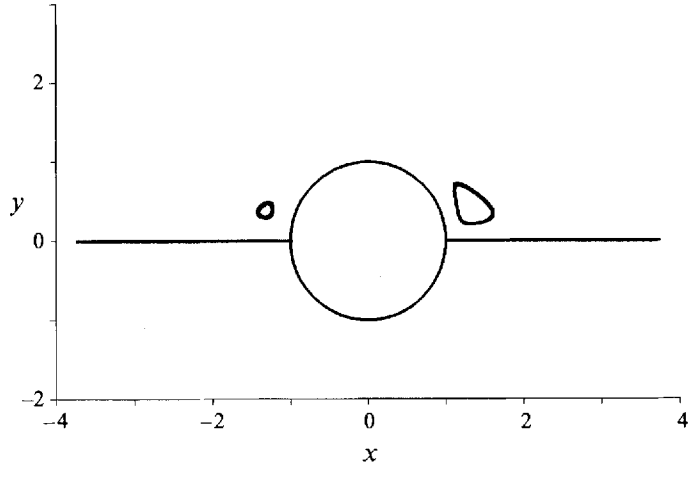

FIGURE 14. Non-symmetric vortex trajectories in the corners of a wing–body combination.

near the lower equilibrium position is plotted in figure 13 for $\Gamma/w = 4.4$ to illustrate this merging.

4.4. *Non-symmetric case*

For the equilibrium positions at the top of the configuration the same considerations as described for the equilibrium near the circular cylinder (§3) apply. The vortices in the corners, however, are not necessarily blown away as they are above a cylinder. The vortices in the corners do not need another free vortex in the neighbourhood that moves symmetrically. The 'capturing action' is in fact accomplished by the mirror vortices which we force to move to fulfil the boundary conditions at the contour. A small disturbance away from the equilibrium position will cause a vortex to start moving around its equilibrium position, while on the other side of the body the vortex may stay close to its equilibrium position and move around it with a different amplitude, only slightly influenced by the vortex at the other side of the body. How much influence there is depends on the amount of shielding that is accomplished by the body. The interesting point is that a single vortex can be captured in a corner.

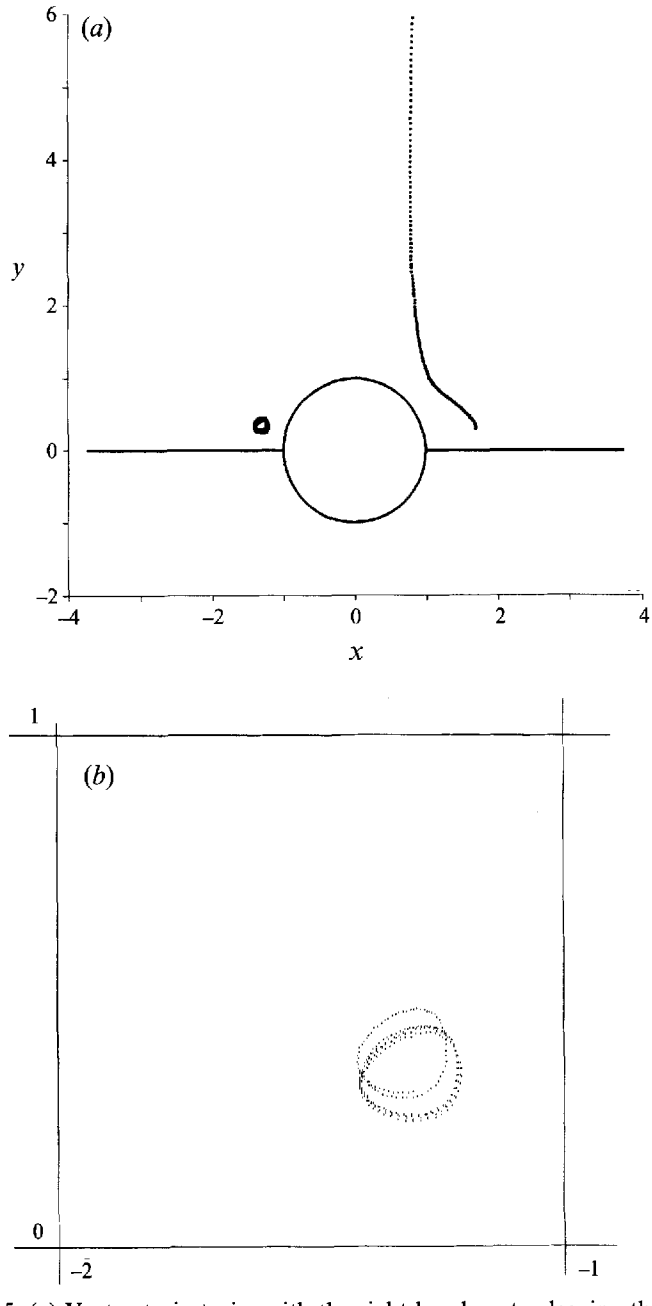

FIGURE 15. (*a*) Vortex trajectories with the right-hand vortex leaving the contour. (*b*) Trajectory of the left-hand vortex of (*a*).

An example of two different almost periodic trajectories on either side of the body is given in figure 14. In this case we have a non-stationary flow field with two slightly different frequencies, which causes beating in the total resulting force and moment on the contour.

In figure 15(*a*) an example is given when the disturbance given to the right-hand vortex is large enough to cause it to be convected away. But the left-hand vortex stays in its orbit round its equilibrium position. The influence of the moving right-hand

vortex on the trajectory of the left-hand vortex is clearly seen in figure 15(*b*). Initially there is a quasi-periodic motion of the left-hand vortex. Ultimately the flow will tend to a periodic situation with a definite vortex trajectory.

5. Concluding remarks

For a vortex in a rectangular corner stagnation flow field equilibrium positions are found, where the vortex velocity equals zero for a certain value of Γ/k. Expressions are derived for these equilibrium positions.

When a vortex in a rectangular corner flow field is given a small disturbance from its equilibrium position, it is found to describe a trajectory around this equilibrium position. This means that a single vortex in a corner stagnation flow field can perform a closed trajectory (rotation) all by itself. This is important because when oscillating forces caused by vortices are present, the explanation is often sought in a system of co-rotating vortices (e.g. Ericsson 1987 and Hall *et al.* 1990), while in this study it is shown that there are equilibrium positions for a vortex in a corner flow field around which the vortex can rotate at a definite frequency on its own.

The periods of the resulting trajectories tend to a definite minimum value when the radius tends to zero. The limit frequencies are derived as a function of the equilibrium position and the magnitude of the flow field (k or w) for a vortex in a rectangular corner, as well as for the equilibrium position of a vortex pair symmetrically placed in the stagnation flow field above a circular cylinder in an upward uniform flow.

The equilibrium of a vortex pair above a circular cylinder in an upward uniform flow is found to be unstable for non-symmetrical disturbances (as already noted by Föppl). This turned out also to be the case for the equilibrium at the top of a wing–body combination. This means that the vortices are carried away with the fluid when a non-symmetrical disturbance occurs. To enforce symmetry, a splitter plate can be placed in the plane of symmetry. Such a splitter plate would (partly) prevent the vorticity being convected away with the upward flow due to non-symmetrical disturbances and thus in fact captures the vortex. In placing a splitter plate one should of course be aware of the possibility of introducing oscillating forces caused by rotating vortices as pointed out in this study.

The equilibrium in the corner of the wing–body junction is found to be neutral. A small displacement from the equilibrium position causes a single vortex to perform a periodic motion (closed trajectory) around its equilibrium position. A second free vortex that symmetrically moves along is not needed to maintain the periodic motion, because the capturing action is accomplished by the 'mirror vortices' representing the boundaries of the corner. This neutral equilibrium is found to disappear for Γ/w greater than a certain value. For these values of Γ/w only the equilibrium above the body exists.

An approximation has been made of the stagnation-point flow fields in the corner of the wing–body junction and on the top of the body. The equilibrium position and frequency belonging to a certain configuration (with wingspace b and body radius c) with a known Γ/w are easily approximated by the derived expressions. Farther away from the stagnation points the equilibrium positions and corresponding frequencies for a certain wing–body combination are calculated numerically.

The present two-dimensional results were constructed in view of possible applications to flows around slender wing–body configurations at an angle of attack with vortices generated by strakes or at the front part of a fuselage. The initial conditions for the two-dimensional flows discussed in this paper can then be related to

the boundary conditions in the three-dimensional flow where the vortices are being generated. Assuming steady flow with respect to the aircraft leads to a steady cross-flow which can be related to the present unsteady solutions by using the simple approximate correspondence

$$\frac{\partial}{\partial t} = U\frac{\partial}{\partial x}, \tag{23}$$

where U is the uniform velocity of the aircraft in the axial direction with respect to the air at rest (figure 1) and x is the coordinate in the axial direction moving with the aircraft. The orbits of the vortex lines would thus lead to steady helical vortices with, of course, a finite radius of curvature and infinite velocity induced on themselves in the direction of the binormal. One might say that in such an application the vortices would immediately break down. Replacing the line vortices by more realistic finite core distributions of vortex filaments leads to finite velocities which, however, may become quite large. It is not quite a straightforward matter to combine such velocities with the velocities obtained in the cross-flows discussed in this paper. Obviously relation (23) would need modification since the axial convection speed of the vortex cores cannot be approximated by the uniform velocity component U and would be dependent on the structure of the inner core and the assumed initial values.

If the three-dimensional vortex-lines are considered to be already present, the velocity of a point vortex in the cross-flow is to be interpreted as the lateral velocity of an infinite straight vortex line in the three-dimensional flow. There would then be oscillating forces on the contour as a result of the changing momentum in the flow field and the resulting changing pressure on the surface.

REFERENCES

BATCHELOR, G. K. 1967 *An Introduction to Fluid Dynamics*. Cambridge University Press

ERICSSON, L. E. 1987 Vortex-induced bending oscillation of a swept wing. *J. Aircraft* **24**, 195–202.

HALL, R. M., ERICKSON, G. E., STRAKA, W. A. *et al.* 1990 Impact of nose-probe-chines on the vortex flows about the F-16C. AIAA-90-0386.

LAMB, H. 1932 *Hydrodynamics*. Dover.

LIGHTHILL, M. J. 1985 *An Informal Introduction to Theoretical Fluid Mechanics*. Clarendon Press.

LIN, C. C. 1941 On the motion of vortices in two dimensions – II. Some further investigations on the Kirchhoff–Routh function. *Nat. Acad. Sci.* **27**, 575–577.

MILNE-THOMSON, L. M. 1967 *Theoretical Hydrodynamics*, 5th edn. MacMillan.

SAFFMAN, P. G. 1992 *Vortex Dynamics*. Cambridge University Press.